

## Highly Reactive Small Molecules

## Preparation and Spectroscopic Studies of FC(O)SSCI

Melina V. Cozzarín,<sup>[a]</sup> Shengrui Tong,<sup>[b]</sup> Mao-Fa Ge,<sup>[b]</sup> Carlos O. Della Védova,<sup>[a]</sup> and Rosana M. Romano<sup>\*[a]</sup>

**Abstract:** The hitherto unknown FC(O)SSCI molecule has been prepared by the reaction of ClC(O)SSCI with TIF under vacuum conditions. The molecule was characterized by its electron-impact mass spectrum, the IR spectrum of a vapour-phase sample, the Raman spectrum of the liquid, and also the matrix-isolated FTIR spectra. FC(O)SSCI is composed of an equilibrium mixture of two conformers, *syn-gauche* and *anti-gauche*, both in the vapour and liquid phases, with an approximate ratio of 80:20.

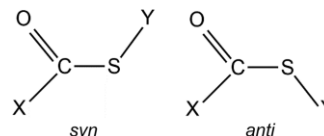
The valence electronic properties of FC(O)SSCI were studied by photoelectron spectroscopy. The first ionization potential was observed at 10.14 eV, and the HOMO was assigned to the non-bonding electron lone pair located on the S atom bonded to the carbonyl group. A decrease in the dihedral angle of the S–S bond after ionization was predicted by quantum chemical calculations.

## Introduction

Sulfenyl chloride compounds, RS–Cl, have been extensively used in organic and inorganic chemical synthesis to transfer the RS– moiety in one-step reactions.<sup>[1–5]</sup> In particular, our research group has prepared different molecular species through the reaction of XC(O)S–Cl (X = halogen). FC(O)SNSO,<sup>[6]</sup> ClC(O)SNSO,<sup>[7]</sup> FC(O)SNCO,<sup>[8]</sup> FC(O)SN,<sup>[9]</sup> FC(O)SCN,<sup>[10]</sup> ClC(O)SCN,<sup>[11]</sup> FC(O)SSCN,<sup>[12]</sup> FC(O)OSO<sub>2</sub>CF<sub>3</sub>,<sup>[13]</sup> ClC(O)OSO<sub>2</sub>CF<sub>3</sub>,<sup>[14]</sup> and FC(O)SSC(O)F<sup>[15]</sup> are examples of molecules synthesized either from FC(O)SCL or ClC(O)SCL.

Besides their important uses as reactants, sulfenyl carbonyl compounds of the type XC(O)SY present very interesting conformational properties. In all the studied molecules, the *syn* conformation prevails (the C=O double bond *syn* with respect to the S–Y single bond, as depicted in Scheme 1). Most of the species with X = F, that is, FC(O)SY, present a second form, with the C=O double bond *anti* with respect to the S–Y single bond (also depicted in Scheme 1), with appreciable abundance at ambient temperature.<sup>[6,16–18]</sup> One exception to this general behaviour was observed for FC(O)SCH<sub>3</sub>, which has only 2 % of the second conformer in equilibrium with the most stable *syn* form, as detected by FTIR spectroscopy after UV/Vis broad-band photolysis of the compound isolated in argon or nitrogen matrices.<sup>[19]</sup> On the other hand, for ClC(O)SY, the difference in energy between the *syn* and *anti* conformers is, in general, larger than

that for the fluorinated derivatives, which results in the observation of the *syn* rotamer only. The first example of an *anti* conformation for a ClC(O)SY molecule was detected by our group in the matrix photochemistry of ClC(O)SBr, isolated in solid Ar, N<sub>2</sub> or Kr.<sup>[20]</sup> In these experiments the vapour of the compound was found to be composed of less than 1 % of the *anti* form, in equilibrium with the more stable *syn* conformer. The *anti* rotamer was unambiguously identified after its formation in a randomization process produced by photolysis of the matrix.



Scheme 1. Representation of the *syn* and *anti* forms of XC(O)SY compounds.

In this paper we present the preparation of the hitherto unknown FC(O)SSCI, a new member of the FC(O)S– family. The presence of a terminal S–Cl single bond turns this species into a potentially useful reactant for chemically transferring the FC(O)SS– unit. The molecule was characterized by electron-impact mass spectrometry. Its conformational equilibrium was investigated by vibrational techniques (FTIR spectroscopy of the vapour phase and as solid in Ar matrix, and Raman spectroscopy of the liquid). The valence electronic properties, of fundamental importance to understanding its chemical reactivity, were studied by gas-phase photoelectron spectroscopy. The experimental results were interpreted with the aid of quantum chemical calculations.

## Results and Discussion

## Preparation of FC(O)SSCI

FC(O)SSCI was obtained by the reaction of ClC(O)SSCI (prepared according to a published procedure)<sup>[21]</sup> with TIF under vacuum

[a] CEQUINOR (UNLP, CCT-CONICET La Plata). Departamento de Química, Facultad de Ciencias Exactas, Universidad Nacional de La Plata, Blvd. 120 No. 1465, CC 962, La Plata (CP 1900), República Argentina  
E-mail: romano@quimica.unlp.edu.ar  
<http://cequinor.quimica.unlp.edu.ar/>

[b] State Key Laboratory for Structural Chemistry of Unstable and Stable Species, Beijing National Laboratory for Molecular Sciences (BNLMS), Institute of Chemistry, Chinese Academy of Sciences, Beijing 100190, Peoples Republic of China

Supporting information for this article is available on the WWW under <http://dx.doi.org/10.1002/ejic.201600966>.

conditions [Equation (1)]. Freshly prepared liquid ClC(O)SSCl (10 mmol) was condensed into a Carius tube, equipped with a Young valve, already containing dried TIF (13 mmol), approximately 30 % in excess with respect to the 1:1 stoichiometric ratio. The reaction mixture was stirred at 20 °C, and the progress of the reaction was monitored by GC–MS and FTIR spectroscopy. The highest yield of FC(O)SSCl, unambiguously recognized by its electron-impact mass spectrum, was observed after 5 h of reaction.



The compound was purified through successive trap-to-trap distillations under vacuum conditions at different temperatures (20, –5, –50 and –196 °C or 20, –20, –80 and –196 °C). The pure compound was retained in the traps at –50 and –20 °C, respectively. The purity of FC(O)SSCl, a yellow liquid at ambient temperature, was confirmed by GC–MS.

### Gas Chromatography–Mass Spectrometry

The gas chromatogram of a CCl<sub>4</sub> solution of the purified sample presented a single peak with a retention time of 3.2 min under the experimental conditions detailed in the Supporting Information. In the electron-impact mass spectrum the parent ion, with its characteristic <sup>35</sup>Cl/<sup>37</sup>Cl isotopic distribution, is observed at *m/z* = 146 and 148, respectively, with an approximate abundance of 57 %. The main fragments are SS<sup>+</sup> (100 %), SSCI<sup>+</sup> (58 %), S<sup>+</sup> (30 %), FCO<sup>+</sup> (24 %), FC(O)SS<sup>+</sup> (21 %), OCS<sup>+</sup> (17 %) and SCl<sup>+</sup> (13 %). It is interesting to note that two ions are formed after an atomic rearrangement: FS<sup>+</sup> (4 %) and FSS<sup>+</sup> (4 %). A complete list of the observed fragments, together with their relative intensities and assignments, is presented in Table S1 of the Supporting Information.

### Computational Conformational Studies

To help in the interpretation of the experimental vibrational and electronic studies, a theoretical investigation of the possi-

ble conformers of FC(O)SSCl was performed. As mentioned in the Introduction, compounds of the formula FC(O)SY usually adopt two different conformations, *syn* (the C=O double bond *syn* with respect to the S–Y single bond) and *anti* (the C=O double bond *anti* with respect to the S–Y single bond), depending upon the energy difference between these two forms of the Y substituent.<sup>[6,16–19]</sup> On the other hand, it is well known that the dihedral angle around the S–S single bond is close to 90° (*gauche*).<sup>[22]</sup>

Three relaxed potential energy scans were performed at the B3LYP/6-311+G\* level of theory. The potential energy curve calculated as a function of the O=C–S–S torsional angle in steps of 10° presents two minima, at 0° (*syn*) and 180° (*anti*), with a *syn/anti* energy barrier of 7.67 kcal mol<sup>–1</sup>. Relaxed potential energy scans of the C–S–S–Cl torsional angle for the two forms were subsequently performed, also in steps of 10°. In both cases the curves present two enantiomeric *gauche* minima with energy barriers of 14.23 (0°) and 8.09 kcal mol<sup>–1</sup> (180°) for the *syn* rotamer and 14.41 (0°) and 8.69 kcal mol<sup>–1</sup> (180°) for the *anti* conformer. The resultant two possible conformations of FC(O)SSCl, *syn-gauche* and *anti-gauche*, were optimized at the B3LYP/6-311+G\*, B3LYP/AUG-cc-pVDZ and MP2/6-311+G\* levels of approximation. Table S2 in the Supporting Information presents the calculated zero-point corrected energies and free-energy differences of the two conformers and their predicted relative populations at ambient temperature. The *syn-gauche* form was predicted to be the most stable one, with a calculated energy difference with respect to the *anti-gauche* conformer of 1.05 (B3LYP/6-311+G\*), 0.89 (B3LYP/AUG-cc-pVDZ) or 1.77 kcal mol<sup>–1</sup> (MP2/6-311+G\*). The relative proportion of the conformers was 80:20, according to the B3LYP/AUG-cc-pVDZ model. The optimized molecular models are shown in Figure 1.

The harmonic and anharmonic vibrational frequencies and also the vertical ionization energies of both conformers were calculated to assist in the interpretation of the vibrational and photoelectron studies, respectively. The results of these calculations will be presented below together with the descriptions and analysis of the respective experiments.

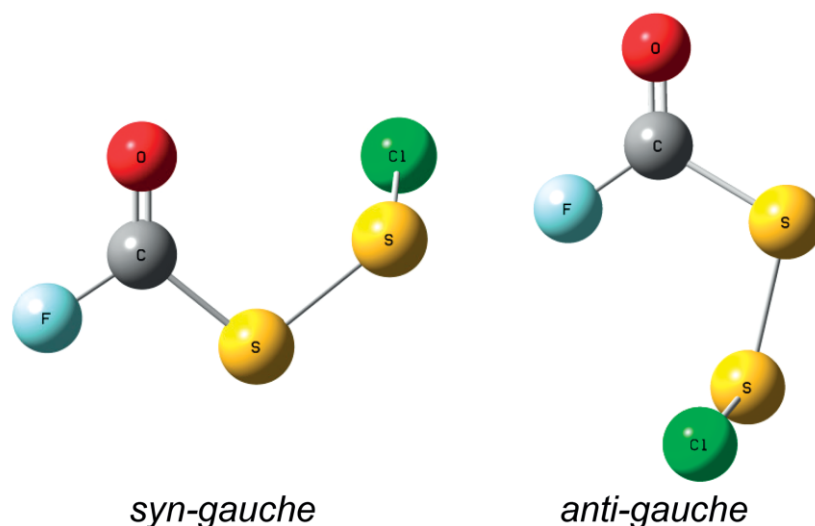


Figure 1. Molecular models of the *syn-gauche* and *anti-gauche* conformers of FC(O)SSCl calculated at the B3LYP/AUG-cc-pVDZ level of theory.

## Vibrational Spectroscopy

The vibrational study of the FC(O)SSCl molecule was performed by analysing the FTIR spectra of a sample in the gas phase at different pressures, the FT-Raman and Raman spectra of the neat liquid, and also the FTIR spectra of Ar-matrix-isolated samples. According to the simulated vibrational spectra of the two conformers, several fundamental normal modes present wavenumber differences larger than the resolution of the experimental spectra, particularly the vibrations assigned to the C=O and C–F stretching modes. A complete list of the anharmonic wavenumbers and IR and Raman relative intensities calculated with the B3LYP/AUG-cc-pVDZ and MP2/6-311+G\* approximation is presented in Table S3 and Table S4 in the Supporting Information for the *syn-gauche* and *anti-gauche* conformers, respectively.

The gas-phase FTIR spectrum and the Raman spectrum of a liquid sample recorded with the 514.5 nm excitation line, shown in Figure 2, present clear evidence of the presence of the two conformers of FC(O)SSCl. The wavenumbers observed in these spectra are collected in Table 1, together with those observed in the Ar-matrix FTIR spectrum in a 1:1000 ratio, the anharmonic

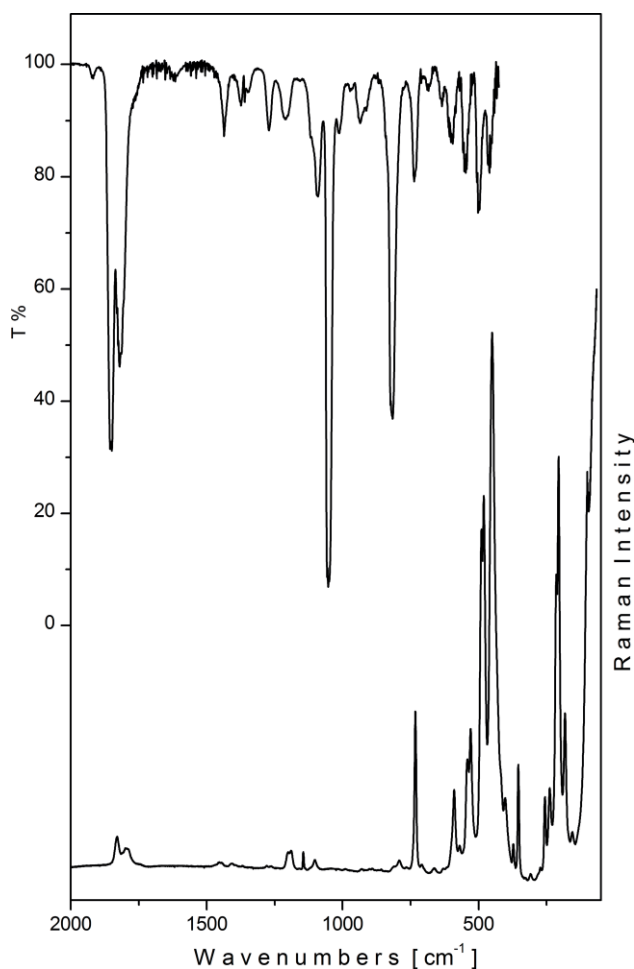


Figure 2. Gas-phase FTIR spectrum of FC(O)SSCl recorded at ca. 6 mbar, resolution of 0.5 cm<sup>-1</sup> and an optical pathlength of 10 cm (top), and Raman spectrum of the liquid recorded with excitation at  $\lambda = 514.5$  nm of an Ar laser with 100 mW.

frequencies calculated at the MP2/6-311+G\* level and tentative assignments based on a comparison with related molecules and predictions of the theoretical simulation.

Table 1. Experimental and calculated vibrational wavenumbers of FC(O)SSCl.

FTIR (gas)	Raman (liq)	Ar matrix	MP2/6-311+G*[a]	Assignment[b]
1855 } 1849 } B	1829	1845.3 } 1842.9 }	1847.1	$\nu(\text{C}=\text{O})_{s-g}$
1830 } 1826 }				$[\nu(\text{C}-\text{F})+\nu(\text{C}-\text{S})]_{a-g}$
1819 } 1812 } A	1793	1822.9 } 1819.4 }	1824.2	$\nu(\text{C}=\text{O})_{a-g}$
1805 }				
	1092	1087.8 } 1086.2 }	1062.4	$\nu(\text{C}-\text{F})_{a-g}$
1057 } 1053 } A	1102	1051.2 } 1048.0 }	1030.0	$\nu(\text{C}-\text{F})_{s-g}$
1049 }		1044.7 }		
	734	735.6	734.2	$\nu(\text{C}-\text{S})_{s-g}$
		734.4	733.7	$\nu(\text{C}-\text{S})_{a-g}$
	548	567.3	640.6	$\delta_{\text{oop}}(\text{C}=\text{O})_{s-g}$
			636.8	$\delta_{\text{oop}}(\text{C}=\text{O})_{a-g}$
		541	530.4	$\nu(\text{S}-\text{S})_{s-g}$
		529	524.9	$\nu(\text{S}-\text{S})_{a-g}$
	499	486.3 } 484.1 }	494.8	$\delta(\text{FCO})_{s-g}$
	458	457.8	487.2	$\nu(\text{S}-^{35}\text{Cl})_{s-g}$
		452.8		$\nu(\text{S}-^{37}\text{Cl})_{s-g}$
			372	$\delta(\text{FCS})_{a-g}$
			353	$\delta(\text{FCS})_{s-g}$
			205	$\delta(\text{SSCl})_{s-g}$
			185	$\delta(\text{SSC})_{s-g}$
			103	$\tau(\text{SSCO})_{s-g}$
			78	$\tau(\text{CSSCl})_{s-g}$

[a] Anharmonic wavenumbers. [b] *s-g* and *a-g* denote bands assigned to the *syn-gauche* and *anti-gauche* conformers, respectively.

In accordance with the theoretical predictions, the  $\nu(\text{C}=\text{O})$  and  $\nu(\text{C}-\text{F})$  fundamental modes of each conformer, among others, are distinguished in the spectra, acting as conformational sensors (see Table 1). The  $\nu(\text{C}=\text{O})$  band of the *syn-gauche* form is observed 40 (in the FTIR spectrum) and 36 cm<sup>-1</sup> (in the Raman spectrum) higher than the corresponding bands of the second form, in good agreement with the 23 cm<sup>-1</sup> difference predicted by the MP2/6-311+G\* approximation. A band-shape analysis of these absorptions in the IR gas-phase spectrum is also an important element for corroborating the assignments. As can be observed in Figure 3, the band assigned to the *syn-gauche* conformer presents a B shape (formed of two branches, PR), whereas the band assigned to the *anti-gauche* form can be identified as an A shape (constituted of three branches, PQ-QR).

The B envelope is in accordance with the orientation of the C=O oscillator with respect to the B axis of inertia in the *syn-gauche* conformer, because the potential energy distribution of the C=O symmetry coordinate for this normal mode is usually close to 100 %, whereas for the *anti-gauche* rotamer, the vibration of this group is quasi-parallel to the A axis of inertia, as depicted in Figure 3. The theoretical PR separations, calculated by using the Seth-Paul procedure, are in good agreement with the observed separations.<sup>[23]</sup>

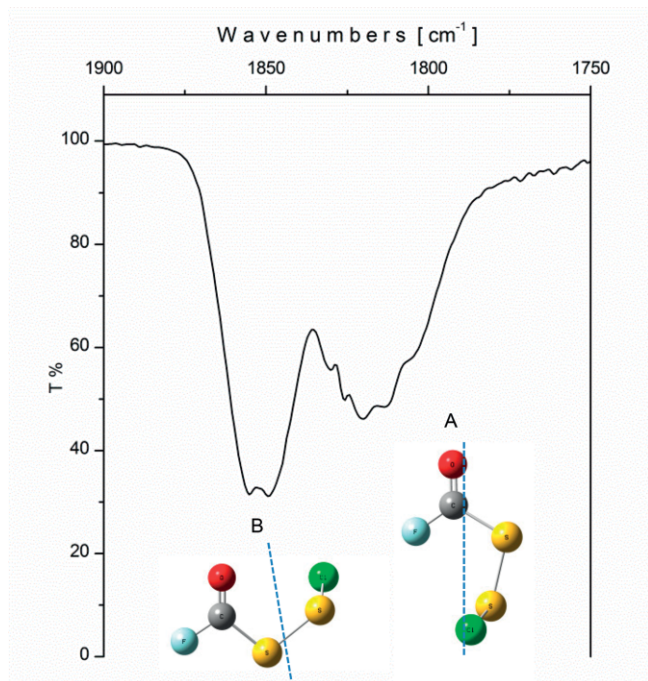


Figure 3. Gas-phase FTIR spectrum of FC(O)SSCl in the carbonyl region.

Close inspection of Figure 3 reveals the presence of a third absorption in the carbonyl energy region, located between the bands of the two conformers, centred at  $1826\text{ cm}^{-1}$ . This signal has been assigned to a combination band of the second conformer,  $[\nu(\text{C-F})+\nu(\text{C-S})]$ , intensified by Fermi resonance with the  $\nu(\text{C=O})$  fundamental mode. This combination band was previously observed in the IR spectrum of the related FC(O)SSCH<sub>3</sub> molecule.<sup>[24]</sup>

The most intense absorption of the IR spectrum, assigned to the  $\nu(\text{C-F})$  vibrational mode, is also indicative of the conformational equilibrium. An A-shaped band centred at  $1053\text{ cm}^{-1}$  is assigned to the *syn-gauche* conformer, in accordance with the expected shape for a structure of this form, with the C-F single bond almost parallel to the A inertial axis. The signal of the second stable form is shifted  $39\text{ cm}^{-1}$  to higher wavenumbers, similarly to the  $32\text{ cm}^{-1}$  shift predicted by the MP2/6-311+G\* method. Comparison of the experimental IR spectrum with a simulated one, constructed by the addition of the calculated IR spectrum of each of the two conformers weighted by their relative abundance, is presented in Figure S1 of the Supporting Information. The experimental spectrum is very well reproduced by the calculations, thereby confirming the conformational equilibrium in the gas phase.

The most intense bands in the Raman spectrum of the liquid, shown in Figure 2, have been assigned to  $\nu(\text{S-S})$ ,  $\nu(\text{S-Cl})$  and  $\delta(\text{SSCl})$ , in agreement with those observed for related molecules, such as ClC(O)SSCl<sup>[21]</sup> and CF<sub>3</sub>SSCl.<sup>[25]</sup> The simulated Raman spectrum of the equilibrium of the two conformers of FC(O)SSCl, presented in Figure S2 of the Supporting Information, is in very good agreement with the experimental spectrum.

The differences in wavenumbers of some of the normal modes in the IR and Raman spectra can account for the intermolecular interactions present in the liquid phase. The most important shifts are observed for the  $\nu(\text{C=O})$  and  $\nu(\text{C-F})$  vibrational modes. For the most stable *syn-gauche* form, the Raman wavenumber of  $\nu(\text{C=O})$  appears  $23\text{ cm}^{-1}$  lower in energy than the same mode in the IR spectrum, which indicates a strong interaction in the liquid phase through this group. On the other hand, the  $\nu(\text{C-F})$  band is observed  $49\text{ cm}^{-1}$  higher in energy in the liquid than in the gas phase, which can be interpreted on the basis that a weakening of the C=O bond should be accompanied by a reinforcement of the C-F single bond.

The FTIR spectrum of FC(O)SSCl isolated in a solid Ar matrix, in a 1:1000 ratio, is characterized by narrow absorption bands, because the interactions are negligible under these conditions, and also because the low temperature eliminates the molecular rotation. The inlet setup allows the freezing of the relative proportion of the conformers at ambient temperature, which transforms matrix-isolation spectroscopy into an ideal technique for studying conformational equilibria. The observed absorptions are included in Table 1, and the FTIR spectrum is presented in Figure S3 of the Supporting Information.

### Photoelectron Spectroscopy

The He-I photoelectron spectrum of the vapour of FC(O)SSCl was recorded between 7 and 20 eV (see Figure 4). To assist in the interpretation of the spectrum, the vertical ionization energies were calculated by using the Outer Valence Green's Function (OVGF) method<sup>[26]</sup> in combination with the 6-31+G\* and aug-cc-pVDZ basis sets. Although there are some examples in the literature of photoelectron spectra that can be correctly evaluated only through the consideration of conformational equilibria,<sup>[27,28]</sup> in the present case the predicted differences in the vertical ionization energies for the two conformers are 40 meV, similar to the spectral resolution of 30 meV. For this reason, the spectrum was interpreted by comparison of the theoretical ionization of the most stable *syn-gauche* conformer only. The experimental ionization potentials, together with the calculated vertical ionizations, are collected in Table 2.

The first ionization potential was observed at 10.14 eV. In accord with the prediction by theoretical calculations, this narrow and well-defined band can be attributed to the ionization of electrons formally located in a nonbonding orbital of the S atom bonded to the FC(O)- group, as schematically depicted in Figure 5. This value is comparable to the 10.7 eV band of the photoelectron spectrum of FC(O)SCl, with the same proposed assignment.<sup>[29]</sup> The second band, at 11.03 eV, was assigned to the lone-pair electrons of the second sulfur atom, bonded to



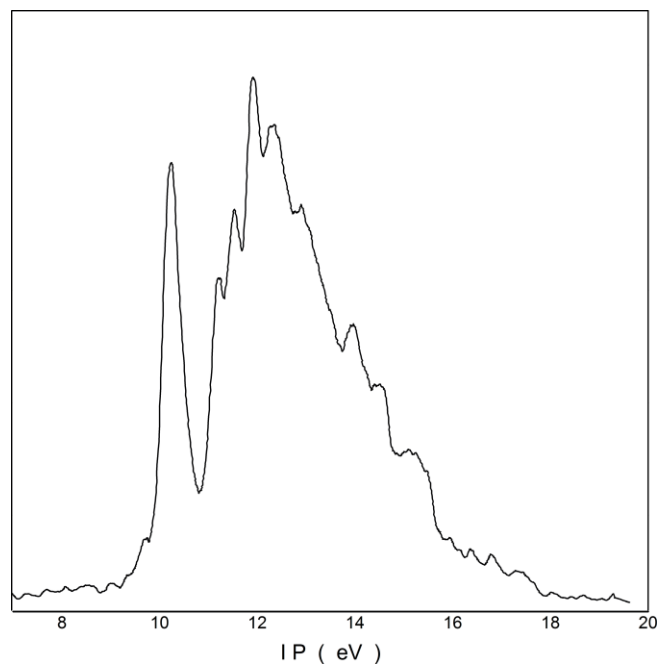


Figure 4. He-I photoelectron spectrum of FC(O)SSCl.

Table 2. Experimental ionization potentials (IP) of FC(O)SSCl, calculated vertical ionization energies ( $E_v$ ) at the OVGf/aug-cc-pVDZ and OVGf/6-31+G\* levels of approximation and molecular orbital characters for the *syn-gauche* conformer.

IP [eV]	$E_v$ [eV] OVGf aug-cc-pVDZ	$E_v$ [eV] OVGf 6-31+G*	MO	Character
10.14	10.16	10.11	36	$n_\pi$ S(S-C)
11.03	11.08	10.95	35	$n_\pi$ S(S-Cl)
11.83	12.01	11.81	34	$n_o$ O
12.53	12.73	12.61	33	$n_\pi$ Cl
13.13	13.43	13.18	32	$n_o$ Cl
13.85	14.33	14.03	31	$\pi$ C=O

Cl. The experimental 0.89 eV energy difference between the two first ionization potentials is in quite good agreement with the 0.92 and 0.84 eV differences predicted at the OVGf/aug-cc-pVDZ and OVGf/6-31+G\* levels, respectively. Not only the energy difference but also the order of these ionizations strongly depends on the substituent. For example, for the related ClC(O)SSCl, the difference is only 0.15 eV,<sup>[21]</sup> whereas for FC(O)SSCH<sub>3</sub>, the order of the ionization energies is inverted, being 9.0 eV for the ionization of  $n$ S(S-CH<sub>3</sub>) electrons and 9.3 eV for  $n$ S[S-C(O)F] electrons.<sup>[29]</sup> The splitting of bands due to the ionization of  $n$ S electrons was also observed for symmetrically substituted disulfides, with an energy difference of 0.30 eV for CH<sub>3</sub>SSCH<sub>3</sub>,<sup>[30]</sup> 0.12 eV for CH<sub>3</sub>C(O)OSSOC(O)CH<sub>3</sub><sup>[31]</sup> and 0.16 eV for CF<sub>3</sub>C(O)OSSOC(O)CF<sub>3</sub>.<sup>[32]</sup>

The third potential, at 11.83 eV, was assigned to the ionization of electrons located in an orbital with  $n_o$ O character, in accord with the theoretical predictions (see Figure 5). This assignment also agrees with those proposed for related molecules [10.74 eV for ClC(O)SCH<sub>2</sub>CH<sub>3</sub>,<sup>[33]</sup> 10.88 eV for ClC(O)SCH<sub>3</sub>,<sup>[34]</sup> 11.3 eV for FC(O)SSCH<sub>3</sub>,<sup>[29]</sup> 11.32 eV for ClC(O)SCL,<sup>[35]</sup> 11.37 eV

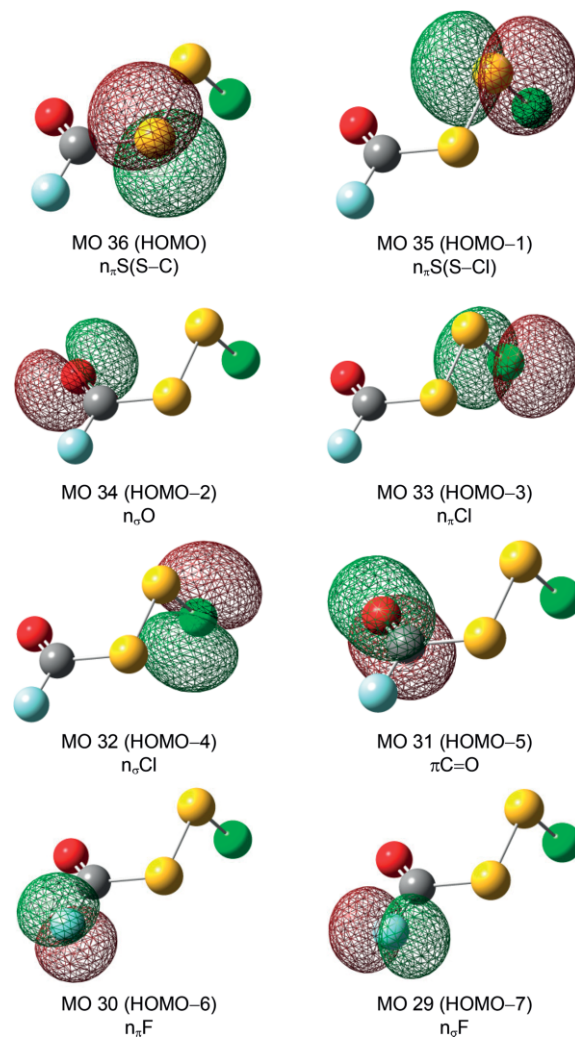


Figure 5. Schematic representations and assignments of the eight highest HOMOs of the *syn-gauche* conformer of FC(O)SSCl calculated with the OVGf/aug-cc-pVDZ approximation.

for FC(O)SCH<sub>2</sub>CH<sub>3</sub>,<sup>[36]</sup> 11.42 eV for ClC(O)SSCl<sup>[21]</sup> and 12.1 eV for FC(O)SCL.<sup>[29]</sup>

The rest of the spectrum is composed of overlapping bands, which were assigned in accord with the predicted ionizations. As can be observed in Table 2, there is very good agreement between the experimental and theoretical values. Between 14 and 16 eV, low-intensity broad bands are observed in the spectrum, which can be assigned to ionizations from the lone-pair electrons of the fluorine atom, as schematically depicted in Figure 5.

The photoionization mass spectrum of FC(O)SSCl after excitation with He-I light was also recorded. The spectrum is composed of three signals, at  $m/z = 28$ , 64 and 100, assigned to the CO<sup>+</sup>, SS<sup>+</sup> and SSCI<sup>+</sup> fragments, respectively. The parent ion was not observed, which denotes the instability of FC(O)SSCl<sup>+</sup> formed after photoionization with 21.22 eV energy.

The structure of FC(O)SSCl after ionization was optimized by using the UB3LYP/6-311+G\* and UMP2/6-311+G\* approximations. The geometrical parameters were compared with those of the corresponding neutral molecule. The most important

change in the geometry of the cation was predicted for the dihedral angle C–S–S–Cl, which decreases from 87.7° (UB3LYP) or 83.7° (UMP2) for the neutral molecule to 39.9° (UB3LYP) or 32.7° (UMP2) for FC(O)SSCI<sup>+</sup>. Similar behaviour was previously reported for the related molecule FC(O)SSCH<sub>3</sub>,<sup>[29]</sup> in which the CSSC dihedral angle drastically changes from *gauche* to *anti* upon ionization, according to HF and MP2 calculations. The Mulliken atomic charges of the cation, calculated by using the UB3LYP/6-311+G\* approximation, are mainly distributed on the SSCI moiety (see Table S5 in the Supporting Information).

## Conclusions

FC(O)SSCI was successfully prepared by the fluorination of ClC(O)SSCI. According to the interpretation of the vibrational studies, based on the FTIR spectrum of the vapour phase (including band-shape analysis), the Raman spectrum of the liquid and the FTIR spectra of the compound isolated in solid Ar, the sample exists as a mixture of two rotamers. The FC(O)SS moiety presents a planar structure in both forms, with the C=O double bond *syn* with respect to the S–S single bond in the more stable conformer, and *anti* in the second rotamer. The theoretical proportion of the rotamers was approximately 80:20, which is in agreement with the relative intensities of the bands observed in the experimental spectra.

The valence electronic properties of FC(O)SSCI were investigated by photoelectron spectroscopy, aided by OVG calculations. The first vertical ionization potential was observed at 10.14 eV and assigned to the ionization of nonbonded electrons formally located on the S atom bonded to the carbonyl group. The structure of the cation formed after ionization was also calculated, and an important change in the S–S dihedral angle was predicted: from *gauche* (ca. 90°) in the neutral molecule to almost 30° in the cationic form.

## Experimental Section

**Sample Preparation:** Reagents and solvents were purchased reagent grade. ClC(O)SSCI was prepared according to a literature procedure<sup>[21]</sup> from freshly synthesized [(CH<sub>3</sub>)<sub>2</sub>CHOC(S)]<sub>2</sub>S.<sup>[37]</sup>

**Gas Chromatography–Mass Spectrometry:** A GC–MS Shimadzu QP-2010 instrument was used to record the mass spectra in CCl<sub>4</sub> solutions. Further details are given in the Supporting Information.

**FTIR Spectroscopy:** The IR spectra in the vapour phase were recorded with a Thermo Nexus Nicolet instrument equipped with either an MCTB or DTGS detector for the ranges 4000–400 and 600–100 cm<sup>-1</sup>, respectively. A 10 cm gas cell with Si or CsI windows was employed, using different pressures of FC(O)SSCI.

**Raman Spectroscopy:** Liquid FT-Raman spectra were recorded with a Bruker IFS66 FT-Raman spectrometer using a FRA 106 Raman accessory in the 3500–100 cm<sup>-1</sup> wavenumber range with a resolution of 4 cm<sup>-1</sup> and 1024 scans. The liquid sample was placed in a sealed 2 mm diameter glass capillary and excited with a 1064 nm Nd-YAG laser. Alternatively, a Raman triple-grating Horiba–Jobin–Yvon T64000 spectrometer system, with a confocal microscope and CCD detector, was also used to record the Raman spectra of the sample. In this case, the sample was placed in a 5 mm diameter glass tube and excited with the 514.5 nm line of an Ar<sup>+</sup> multi-

line coherent laser. The wavenumbers were calibrated by using the 459 cm<sup>-1</sup> band of CCl<sub>4</sub>.

**Matrix Isolation Spectroscopy:** A gaseous mixture of FC(O)SSCI and argon, in an approximately 1:1000 ratio, was prepared by standard manometric methods. The Ar gas (AGA) was passed through a trap cooled to –90 °C to retain possible traces of impurities. The mixture was then deposited on a CsI window cooled to ca. 10 K by means of a Displex closed-cycle refrigerator (SHI-APD Cryogenics, model DE-202) using the pulse deposition technique.<sup>[38–40]</sup> FTIR spectra of the matrix sample were recorded at resolutions of 0.5 and 0.125 cm<sup>-1</sup> with 256 scans using a Nexus Nicolet instrument equipped with either an MCTB or a DTGS detector (for the ranges 4000–400 or 600–180 cm<sup>-1</sup>, respectively).

**Photoelectron Spectroscopy:** The photoelectron spectrum was recorded with a double-chamber UPS-II machine, which was designed specifically to detect transient species as described elsewhere,<sup>[41,42]</sup> at a resolution of ca. 30 meV indicated by the standard Ar<sup>+</sup>(<sup>2</sup>P<sub>3/2</sub>) photoelectron band. The experimental vertical ionization energies were calibrated with methyl iodide.

**Computational Calculations:** The quantum chemical calculations were performed by using the Gaussian 03 program system.<sup>[43]</sup> Geometry optimizations were sought by using standard gradient techniques by simultaneous relaxation of all the geometrical parameters. The calculated vibrational properties correspond in all cases to potential energy minima for which no imaginary vibrational frequency was found. The vertical ionization energies (*E<sub>v</sub>*) were calculated by using the OVGf/aug-cc-pVDZ and OVGf/6-31+G\* levels of approximation.

## Acknowledgments

This work was supported by funds from the Agencia Nacional Científica y Tecnológica ANPCyT (PICT11-0647 and PICT14-3266), the Facultad de Ciencias Exactas of the Universidad Nacional de La Plata (UNLP-11/X684) and the Consejo Nacional de Investigaciones Científicas y Técnicas CONICET (PIP-0352).

**Keywords:** Sulfides · Photoelectron spectroscopy · Conformation analysis · Vibrational spectroscopy · Matrix isolation

- [1] G. Reginato, B. Pezzati, A. Ienco, G. Manca, A. Rossin, A. Mordini, *J. Org. Chem.* **2011**, *76*, 7415–7422.
- [2] C. Nativib, G. Palioa, M. Taddeia, *Tetrahedron Lett.* **1991**, *32*, 1583–1586.
- [3] A. Haas, J. Helmbrecht, W. Klug, B. Koch, H. Reinke, J. Sommerhoff, *J. Fluorine Chem.* **1974**, *3*, 383–395.
- [4] C. O. Della Védova, R. M. Romano, T. Heß, *Spectrochim. Acta* **1993**, *49A*, 1047–1053.
- [5] R. M. Romano, C. O. Della Védova, A. Pfeiffer, H.-G. Mack, H. Oberhammer, *J. Mol. Struct.* **1998**, *446*, 127–135.
- [6] H.-G. Mack, H. Oberhammer, C. O. Della Védova, *J. Mol. Struct.* **1992**, *265*, 347–357.
- [7] C. O. Della Védova, *J. Mol. Struct.* **1992**, *274*, 9–23.
- [8] K. I. Gobbato, S. E. Ulic, C. O. Della Védova, H.-G. Mack, H. Oberhammer, *Chem. Phys. Lett.* **1997**, *266*, 527–532.
- [9] C. O. Della Védova, H.-G. Mack, *J. Chem. Soc. Faraday Trans.* **1995**, *91*, 231–235.
- [10] L. A. Ramos, S. E. Ulic, R. M. Romano, M. F. Erben, C. W. Lehmann, E. Bernhardt, H. Beckers, H. Willner, C. O. Della Védova, *Inorg. Chem.* **2010**, *49*, 11142–11157.
- [11] L. A. Ramos, S. E. Ulic, R. M. Romano, M. F. Erben, Y. V. Vishnevskiy, C. G. Reuter, N. W. Mitzel, H. Beckers, H. Willner, X. Zeng, E. Bernhardt, M. Ge, S. Tong, C. O. Della Védova, *J. Phys. Chem., Part A* **2013**, *117*, 2383–2399.

- [12] S. Tong, L. Du, L. Yao, M. Ge, C. O. Della Védova, *Eur. J. Inorg. Chem.* **2008**, 3987–3995.
- [13] C. O. Della Védova, A. J. Downs, V. P. Novikov, H. Oberhammer, S. Parsons, R. M. Romano, A. Zawadski, *Inorg. Chem.* **2004**, *43*, 4064–4071.
- [14] C. O. Della Védova, A. J. Downs, E. Moschioni, S. Parsons, R. M. Romano, *Inorg. Chem.* **2004**, *43*, 8143–8149.
- [15] H.-G. Mack, C. O. Della Védova, H. Oberhammer, *J. Phys. Chem.* **1992**, *96*, 9215–9217.
- [16] H.-G. Mack, H. Oberhammer, C. O. Della Védova, *J. Phys. Chem.* **1991**, *95*, 4238–4241.
- [17] C. O. Della Védova, *J. Raman Spectrosc.* **1989**, *20*, 729–734.
- [18] H.-G. Mack, C. O. Della Védova, H. Oberhammer, *Angew. Chem. Int. Ed. Engl.* **1991**, *30*, 1145–1146; *Angew. Chem.* **1991**, *103*, 1166.
- [19] R. M. Romano, C. O. Della Védova, A. J. Downs, *Chem. Eur. J.* **2007**, *13*, 8185–8192.
- [20] R. M. Romano, C. O. Della Védova, A. J. Downs, T. M. Greene, *J. Am. Chem. Soc.* **2001**, *123*, 5794–5801.
- [21] Y. A. Tobón, M. V. Cozzarín, W. G. Wang, M. F. Ge, C. O. Della Védova, R. M. Romano, *J. Phys. Chem. A* **2011**, *115*, 10203–10210.
- [22] L. C. Juncal, Y. A. Tobón, O. E. Piro, C. O. Della Védova, R. M. Romano, *New J. Chem.* **2014**, *38*, 3708–3716.
- [23] W. A. Seth-Paul, *J. Mol. Struct.* **1969**, *3*, 403–417.
- [24] C. O. Della Védova, *Spectrochim. Acta* **1991**, *47A*, 1619–1626.
- [25] C. O. Della Védova, *J. Raman Spectrosc.* **1989**, *20*, 279–282.
- [26] L. S. Cederbaum, W. Domcke, *Adv. Chem. Phys.* **1977**, *36*, 205–344.
- [27] M. S. Deleuze, W. N. Pang, A. Salam, R. C. Shang, *J. Am. Chem. Soc.* **2001**, *123*, 4049–4061.
- [28] F. Morini, S. Knippenberg, M. S. Deleuze, B. Hajgató, *J. Phys. Chem. A* **2010**, *114*, 4400–4417.
- [29] M. F. Erben, C. O. Della Védova, *Inorg. Chem.* **2002**, *41*, 3740–3748.
- [30] K. Kimura, K. Osatune, *Bull. Chem. Soc. Jpn.* **1975**, *48*, 2421–2427.
- [31] L. Du, L. Yao, M. Ge, *J. Phys. Chem. A* **2007**, *111*, 11787–11792.
- [32] X. Zeng, M. F. Ge, Z. Sun, D. Wang, *J. Phys. Chem. A* **2006**, *110*, 5685–5691.
- [33] L. Rodríguez Pirani, M. F. Erben, M. Geronés, C. Ma, M. Ge, R. M. Romano, R. Cavasso Filho, C. O. Della Védova, *J. Phys. Chem. A* **2011**, *115*, 5307–5318.
- [34] M. Geronés, M. F. Erben, M. Ge, R. L. Cavasso Filho, R. M. Romano, C. O. Della Védova, *J. Phys. Chem. A* **2010**, *114*, 8049–8055.
- [35] M. Geronés, M. F. Erben, R. M. Romano, C. O. Della Védova, L. Yao, M. Ge, *J. Phys. Chem. A* **2008**, *112*, 2228–2234.
- [36] L. S. Rodríguez Pirani, M. F. Erben, M. Geronés, R. M. Romano, R. Cavasso-Filho, C. Ma, M. Ge, C. O. Della Védova, *J. Phys. Chem. A* **2014**, *118*, 5950–5060.
- [37] G. S. Whitby, F. R. S. C. Gallay, *Trans. R. Soc. Can.* **1929**, *23*, 20–24.
- [38] I. R. Dunkin in *Matrix-Isolation Techniques: A Practical Approach*, Oxford University Press, New York, **1998**.
- [39] M. J. Almond, A. J. Downs, *Adv. Spectrosc.* **1989**, *17*, 1–511.
- [40] R. N. Perutz, J. J. J. Turner, *J. Chem. Soc. Faraday Trans. 2* **1973**, *69*, 452–461.
- [41] L. Yao, M. Ge, W. Wang, X. Zeng, Z. Sun, D. Wang, *Inorg. Chem.* **2006**, *45*, 5971–5975.
- [42] L. Du, L. Yao, X. Zeng, M. Ge, D. Wang, *J. Phys. Chem. A* **2007**, *111*, 4944–4949.
- [43] M. J. Frisch, G. W. Trucks, H. B. Schlegel, G. E. Scuseria, M. A. Robb, J. R. Cheeseman, J. A. Montgomery Jr., T. Vreven, K. N. Kudin, J. C. Burant, J. M. Millam, S. S. Iyengar, J. Tomasi, V. Barone, B. Mennucci, M. Cossi, G. Scalmani, N. Rega, G. A. Petersson, H. Nakatsuji, M. Hada, M. Ehara, K. Toyota, R. Fukuda, J. Hasegawa, M. Ishida, T. Nakajima, Y. Honda, O. Kitao, H. Nakai, M. Klene, X. Li, J. E. Knox, H. P. Hratchian, J. B. Cross, V. Bakken, C. Adamo, J. Jaramillo, R. Gomperts, R. E. Stratmann, O. Yazyev, A. J. Austin, R. Cammi, C. Pomelli, J. W. Ochterski, P. Y. Ayala, K. Morokuma, G. A. Voth, P. Salvador, J. J. Dannenberg, V. G. Zakrzewski, S. Dapprich, A. D. Daniels, M. C. Strain, Ö. Farkas, D. K. Malick, A. D. Rabuck, K. Raghavachari, J. B. Foresman, J. V. Ortiz, Q. Cui, A. G. Baboul, S. Clifford, J. Cioslowski, B. B. Stefanov, G. Liu, A. Liashenko, P. Piskorz, I. Komaromi, R. L. Martin, D. J. Fox, T. Keith, M. A. Al-Laham, C. Y. Peng, A. Nanayakkara, M. Challacombe, P. M. W. Gill, B. Johnson, W. Chen, M. W. Wong, C. Gonzalez, J. A. Pople, *Gaussian 03*, revision B.05, Gaussian, Inc., Pittsburgh, PA, **2003**.

Received: August 4, 2016

Published Online: November 30, 2016